Investigation of clustering in ^{14}N nuclei by means of relativistic-multifragmentation processes

Shchedrina Tatiana,
VBLHE, JINR

Introduction

- The results of investigations of inelastic interactions of ^{14}N nuclei at energy 2.1 GeV per nucleon are presented.
- The main features of these interactions: mean free path, isotopic structure of fragments and fragmentation channels are measured.
- An identification of singly charged fragments was performed. The method is based on the measurements of the relative multiple Coulomb scattering.
- An invariant approach to analysing the fragmentation of relativistic ^{14}N nuclei in emulsion is represented.
- New data for ^{14}N nuclei are extracted from a minor portion of the processed material. It enables one only to outline promising approaches to future analysis.

Experiment

P_0	2.86 GeV/c
L_Σ	70.41 m
Total number of inelastic interactions, including ‘white’ stars	540 25
Mean free path for inelastic interactions	0.13 m

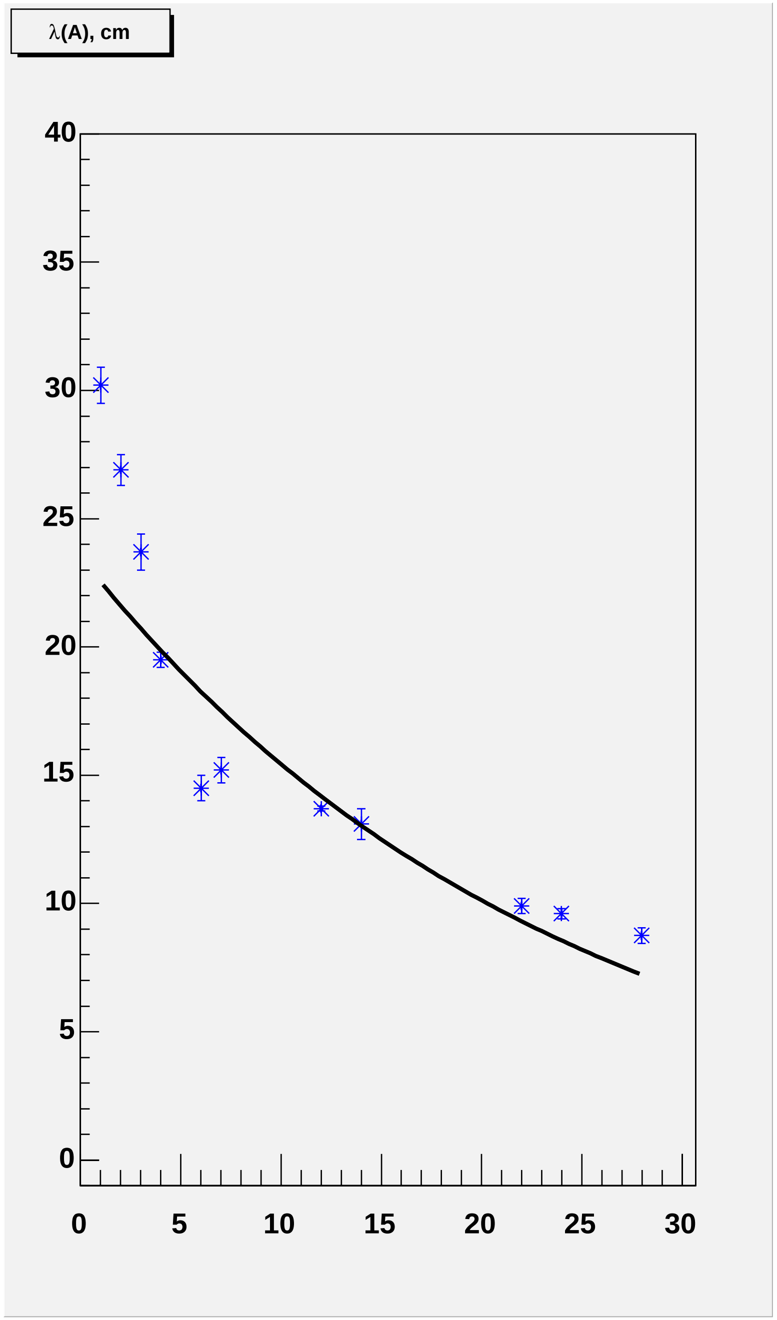

Projectile	P_0, A GeV/c	$\lambda_{experim}$, cm
P	4.5	30.2 ± 0.7
^{2}H	9.4	26.9 ± 0.6
^{3}He	2.7	23.7 ± 0.7
^{4}He	4.5	19.5 ± 0.3
^{6}Li	4.5	14.1 ± 0.4
^{12}C	4.5	13.7 ± 0.5
^{14}N	2.9	13.1 ± 0.6
^{16}O	4.5	13.0 ± 0.5

Mean range of free path with respects to inelastic interactions in the photoemulsion as a function of the projectile mass number. The curve represents the fit obtained within the geometric model.

The charge-topology distribution of 25 ‘white’ stars and 36 interactions with target fragmentation in the dissociation of ^{14}N nuclei at energy 2.1 GeV per nucleon

Z_{fr}	6	5	5	4	3	3	—	—
$N_{z=1}$	1	—	2	1	4	2	3	1
$N_{z=2}$	—	1	—	1	—	1	2	3
$N_{white\ star}$ in percentage terms	6 24%	2 8%	3 12%	1 4%	1 4%	1 4%	1 4%	10 40%
$N_{with\ targ.\ fragm.}$ in percentage terms	10 28%	2 5.7%	1 2.8%	3 8.4%	—	—	4 11.1%	16 44%
N_{total} in percentage terms	16 26%	4 7%	4 7%	4 7%	1 1.5%	1 1.5%	5 8%	26 43%

Example of the peripheral dissociation of ^{14}N nuclei at energy 2.1 GeV per nucleon in emulsion

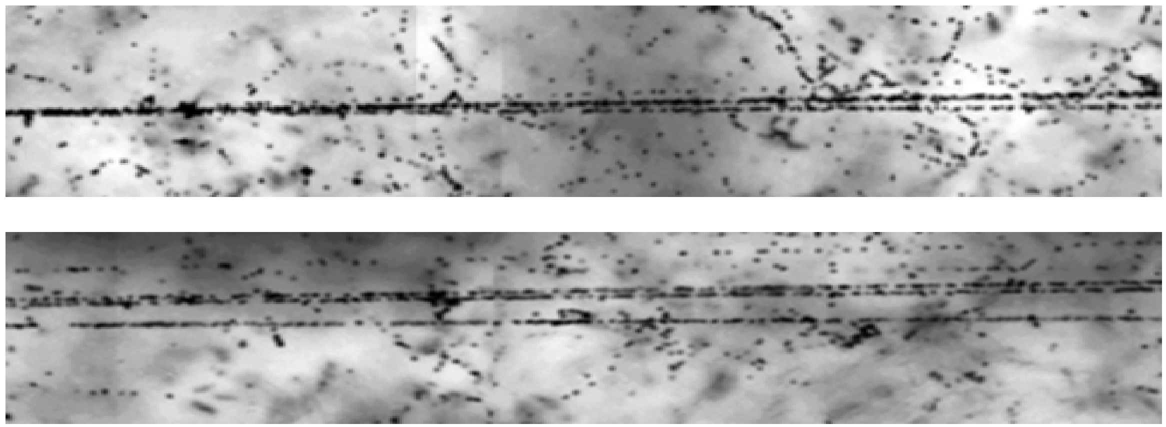

The upper photograph shows the interactions vertex and a jet of fragments within a narrow angular cone. An intense track on the upper photograph (the second one from top to bottom) is identified as a pair of Z=2 fragments that occurs in a very narrow angular cone and which corresponds to the decay of ^{8}Be nucleus. Upon a shift in the direction of the jet of fragments (lower photograph), one can distinguish three He and one H fragments.
The three-dimensional image of events was reconstructed as a plane projection with the aid of an automated microscope entering into the composition of the PAVIKOM complex at the Lebedev Institute of Physics (Moscow).

Example of the peripheral dissociation of ^{14}N nuclei at energy 2.1 GeV per nucleon in emulsion

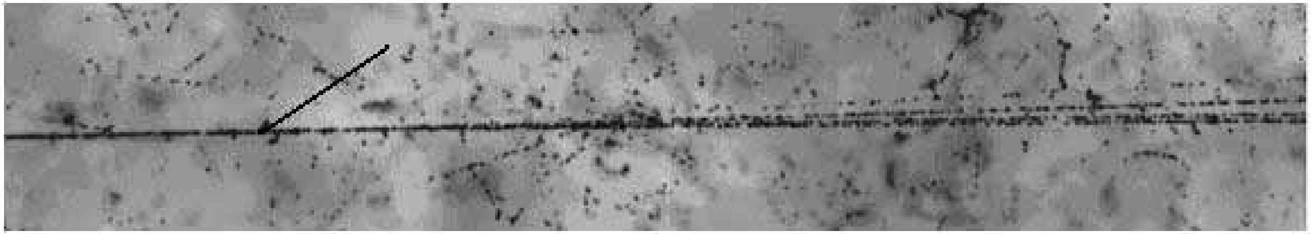

The photograph shows the interaction vertex and a jet of fragments within a narrow angular cone and one target-nucleus fragment.
The three-dimensional image of events was reconstructed as a plane projection with the aid of an automated microscope entering into the composition of the PAVIKOM complex at the Lebedev Institute of Physics (Moscow).

The dominant fragmentation channels

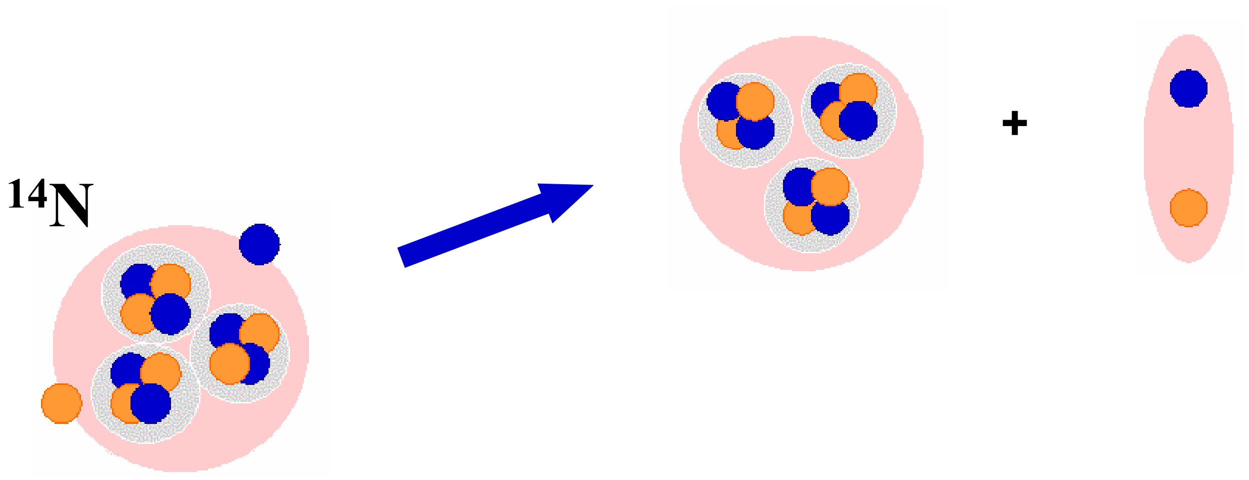

The dominant fragmentation channels

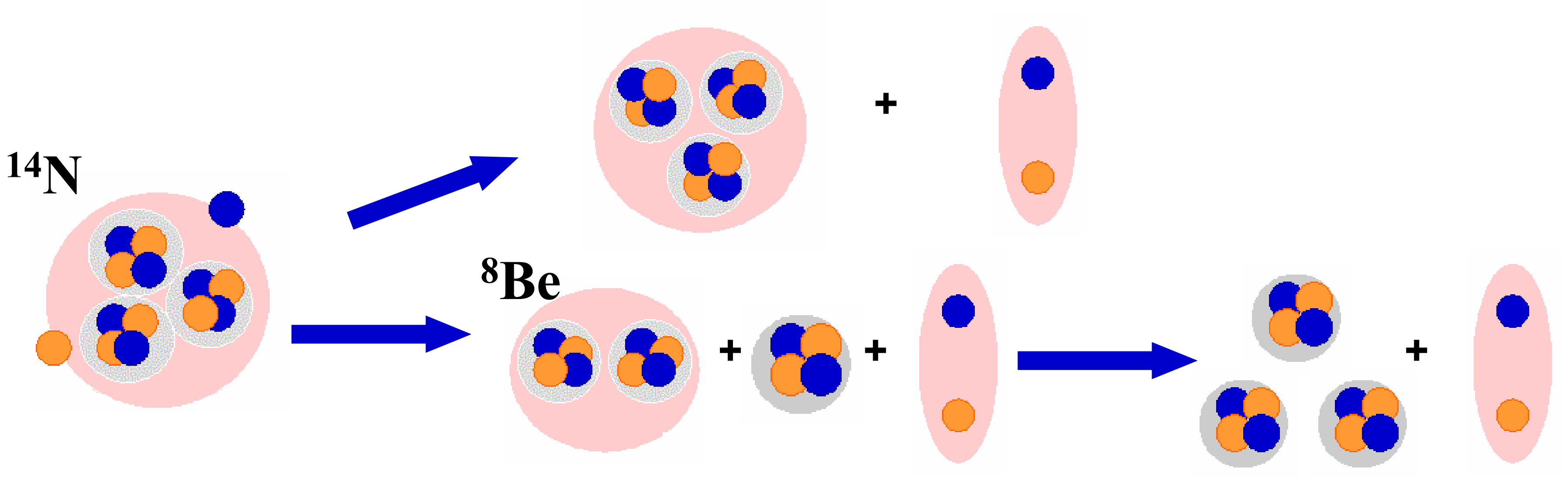

The dominant fragmentation channels

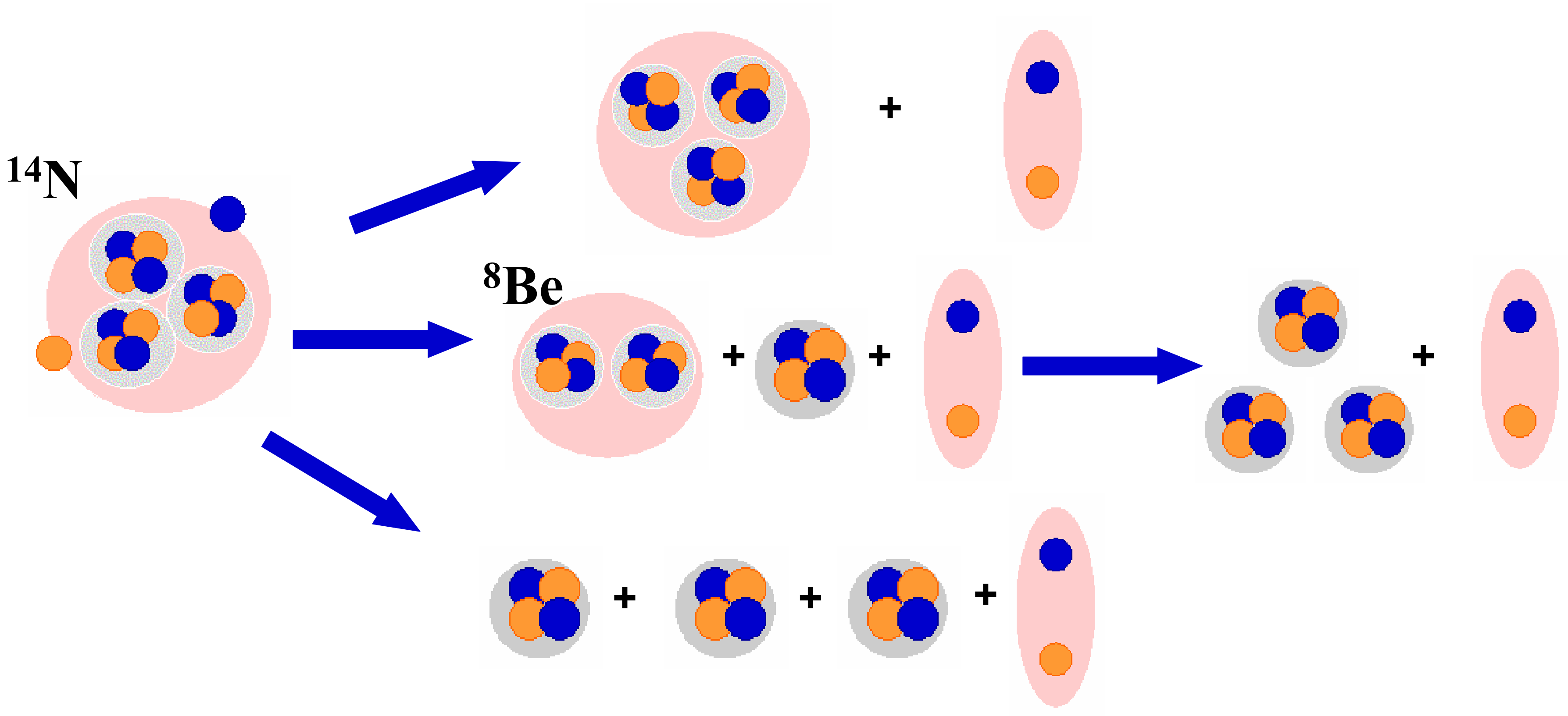

The multiple Coulomb scattering theory

$$P\beta c = \frac{Z_f K t^{3/2}}{573\overline{D}}$$

where **P** – the fragment momentum

$\mathbf{Z_f}$ – the fragment charge

βc – velocity

K – ‘‘scattering const’’

t – the length of a cell

D – the mean deviation

Pβc distribution for singly charged ^{14}N fragments

P_0 =2.86 GeV/c

Pp=2.6 GeV/c

Pd=5.6 GeV/c

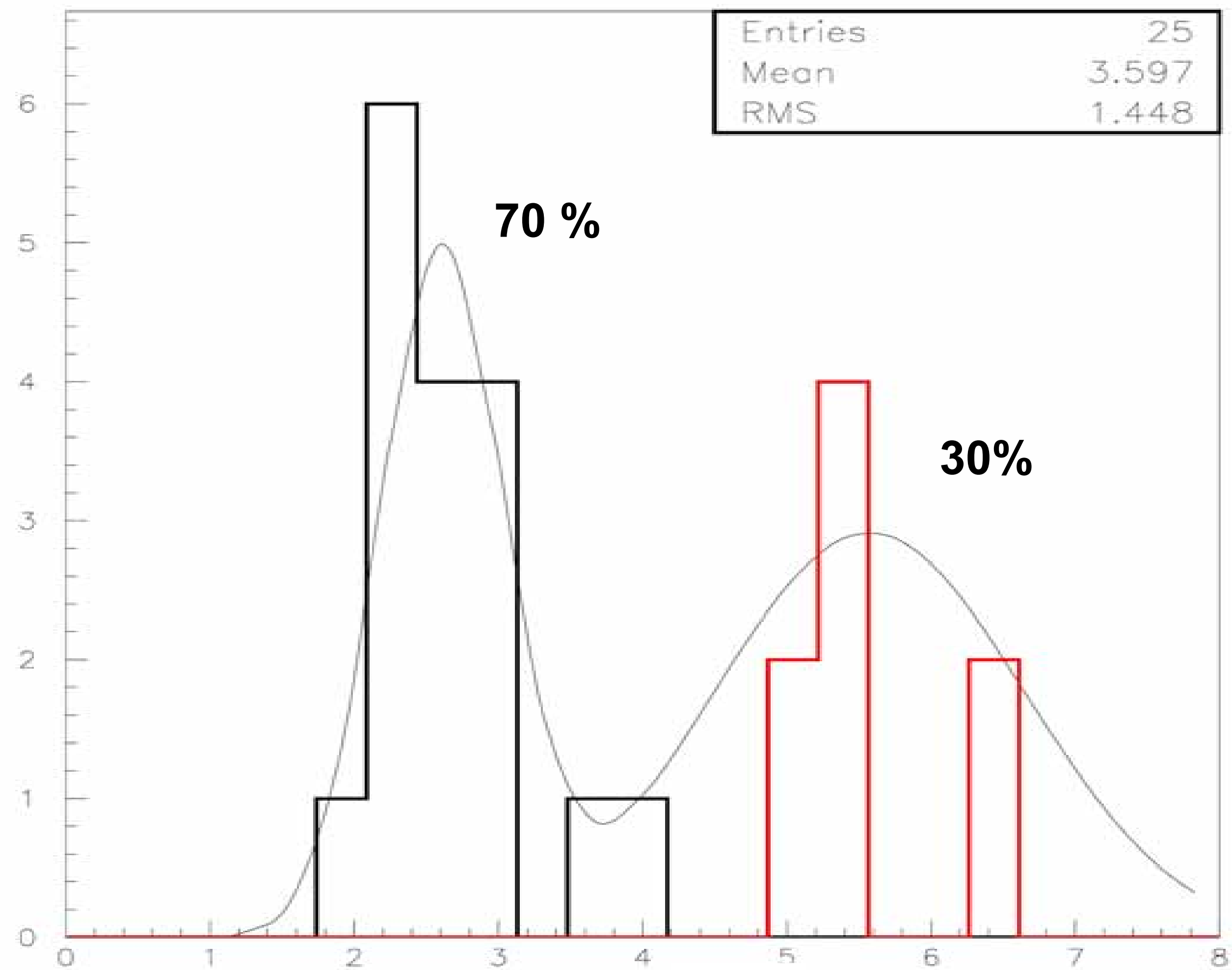

Pβc, GeV/c

The ratio of protons to deuterons of projectile ^{6}Li, ^{10}B и ^{14}N

^{6}Li $(He + p)/(He + d) \approx 1$

^{10}B $(2*He + p)/(2*He + d) \approx 1$

^{14}N $(3*He + p)/(3*He + d) \approx 2:1$

Angular distributions of alpha-particles for channel $^{14}N \rightarrow 3\alpha$ + singly charged particle

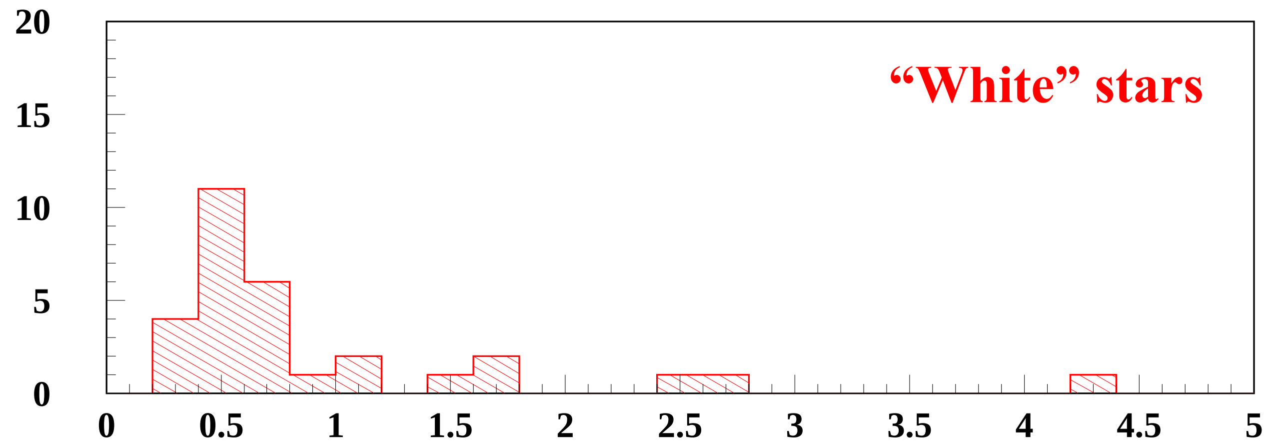

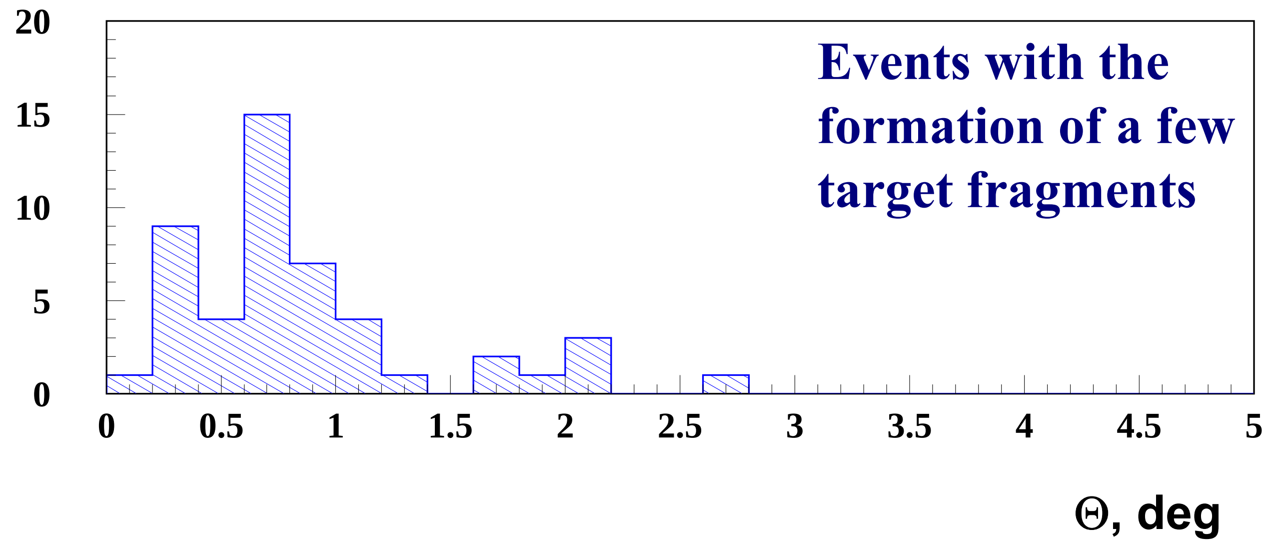

P_t- and θ-distributions of doubly charged fragments for the $^{14}N \rightarrow 3\alpha$ fragmentation channel

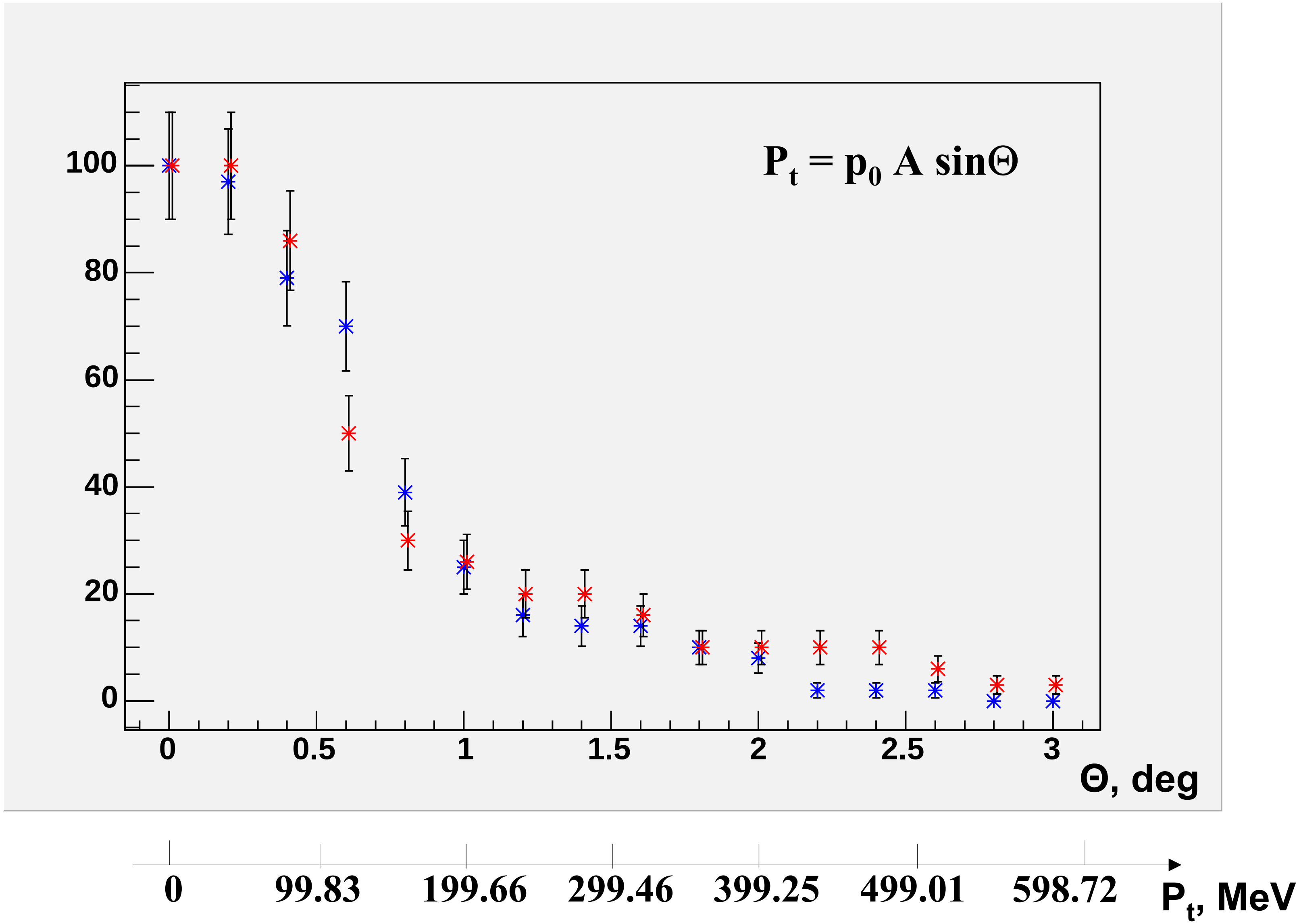

(P_t) θ-distribution of doubly charged fragments for the $^{14}N \rightarrow 3\alpha$ fragmentation channel

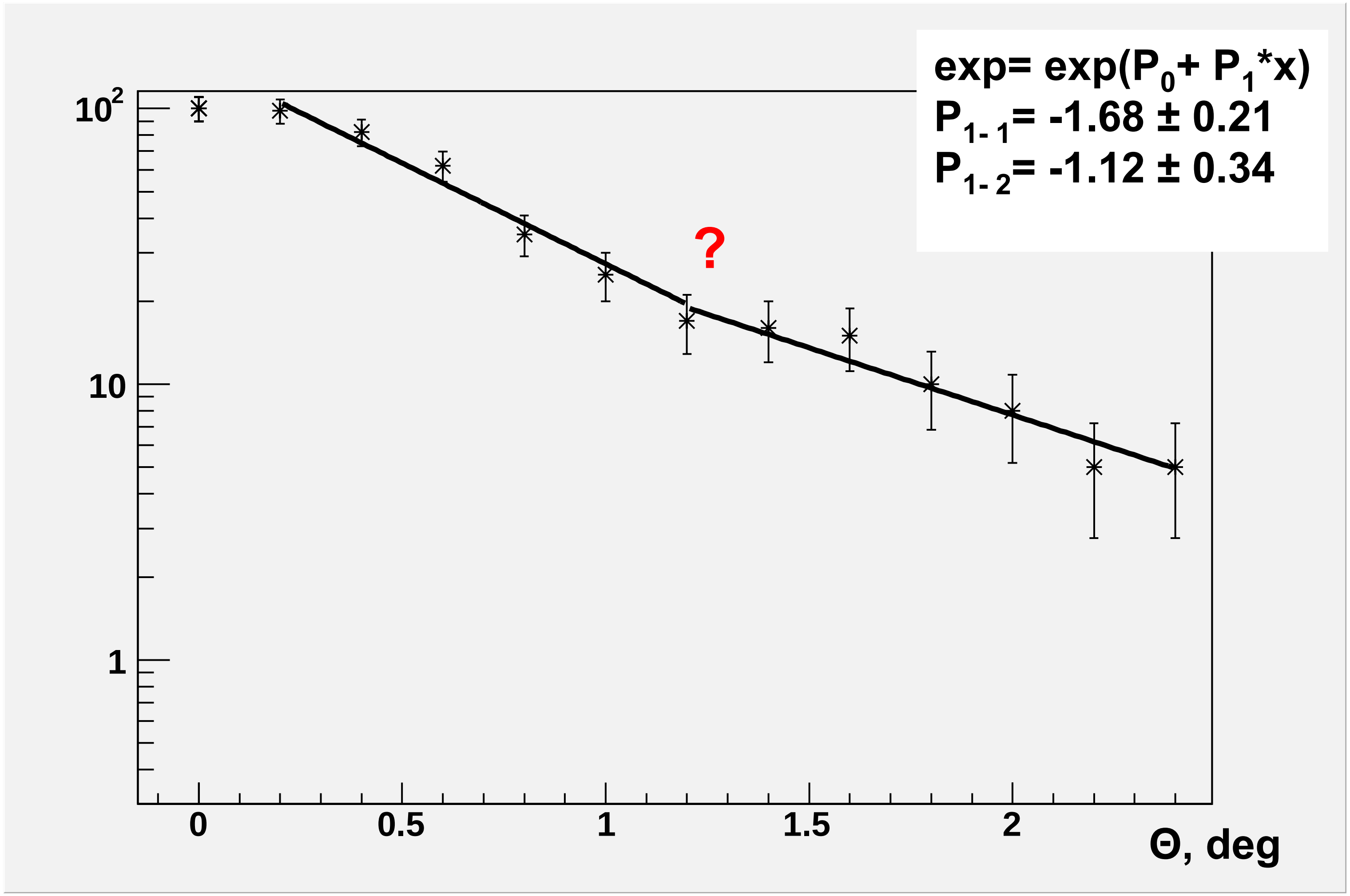

Distributions in the opening angle between fragment pairs for the $^{14}N \to 3\alpha$ fragmentation channel at an energy of 2.1 A GeV

$^{14}N \to \alpha\ ^{8}Be + s$

$Q_{ij} \cong 3 * 10^{-3}$ rad

$^{8}Be\ (0, 0^{+})$

$W \cong 10\ \%$

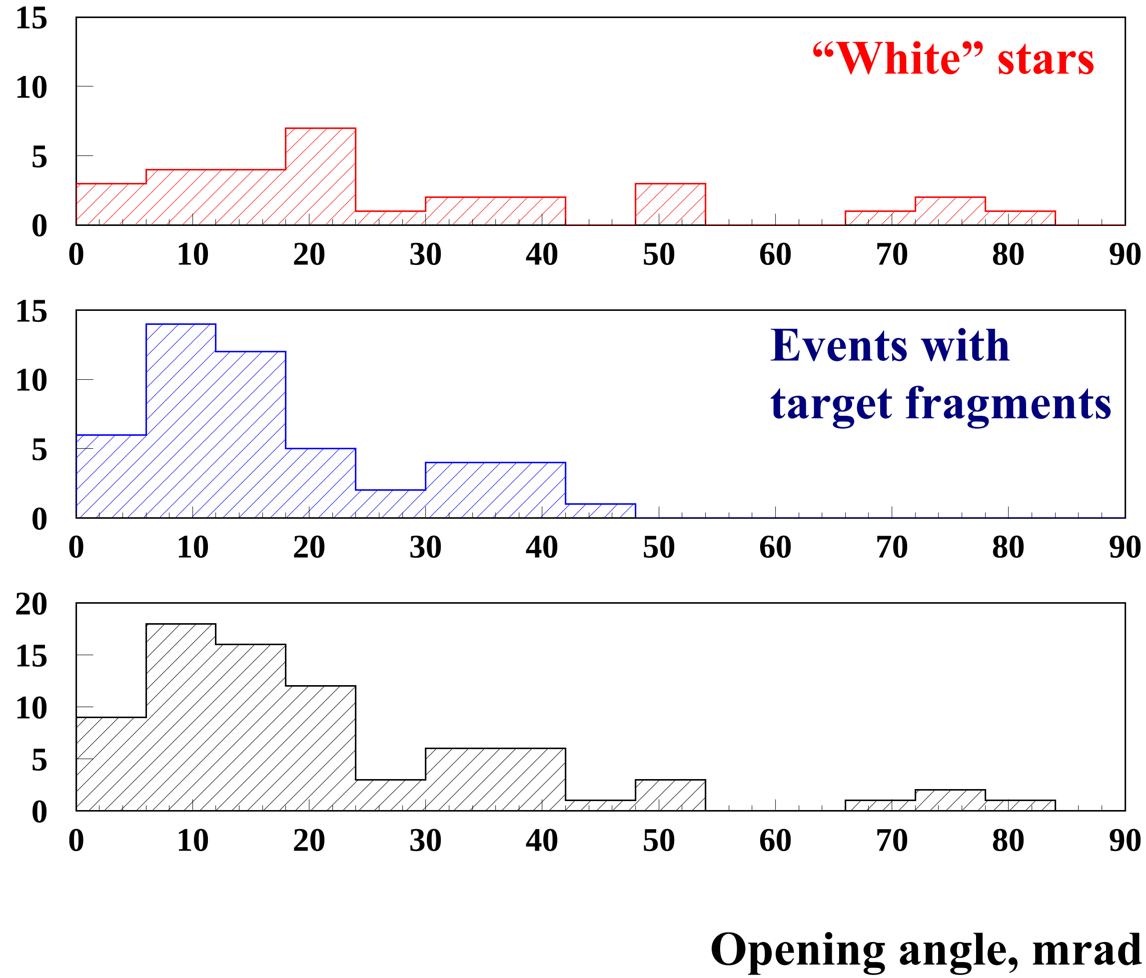

Distribution in invariant excitation energy for the $^{14}N \rightarrow 3\alpha$ channel at an energy of 2.1 A GeV with respects to the ground state of the nucleus ^{12}C

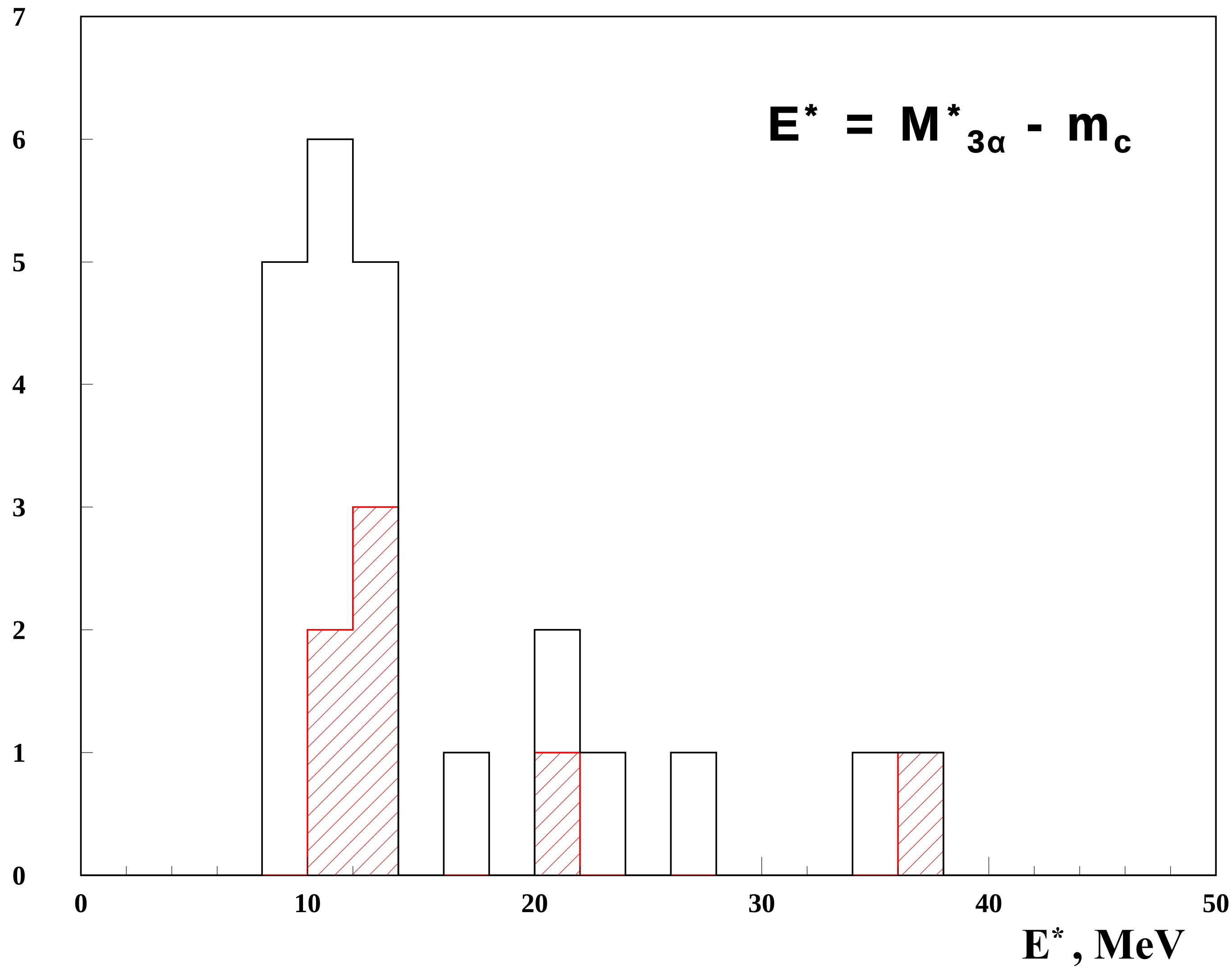

Energy Level Diagram

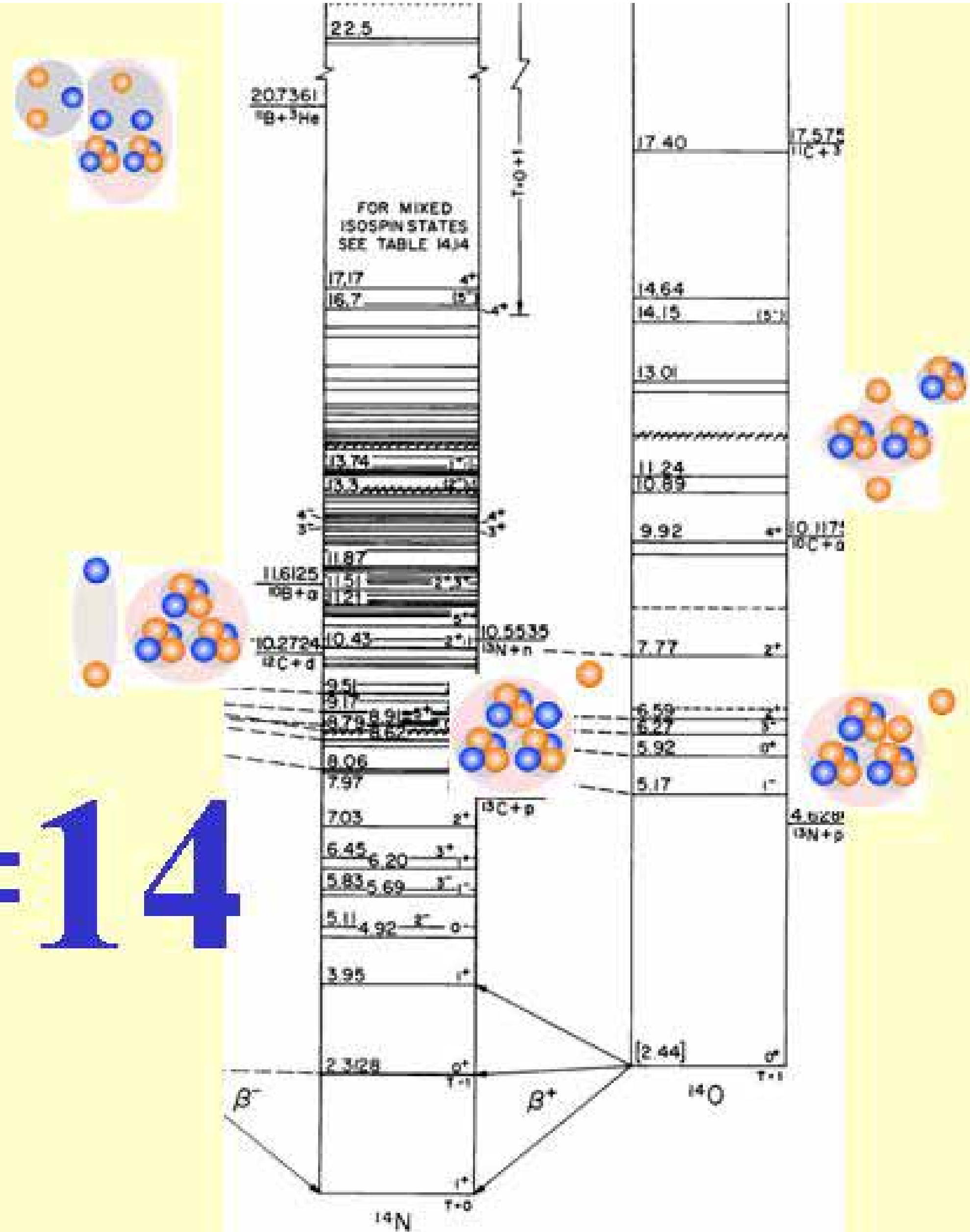

A=14

Summary

- The peculiarities of the production of extremely light nuclei (p, d, alpha), originating from the multifragmentation processes are explored.
- The 'white' stars and peripheral dissociation with the formation of few target-nucleus fragments were studied. Mean free path, isotopic structure of fragments and fragmentation channels are measured for this kind of events. There is an indication of a leading role of the $3\alpha+p$ and $3\alpha+d$ configurations. The 6+1 configuration seems to contribute considerably.
- Preliminary data of multiple Coulomb scattering measurements of singly charged fragments indicate that the ratio of protons to deuterons is approximately as 2:1.
- In the present talk use is made of an invariant approach to analysing the nuclei fragmentation. Estimation of excitation scale for generation 3α-systems is represented. It's indicated that there is a concentration of events in the region of very low energy. According to current statistics, the percentage of interactions in the range from 10 to 14 MeV is 80 %.
- The ^{8}Be yield in the fragmentation of a relativistic ^{14}N nucleus at the energy 2.1 A GeV amounts to about 10 %.
- Gathering of events on the interactions of ^{14}N nuclei at the energy 2.1 A GeV continues now in order to increase statistics by the order of magnitude higher than in the present report.

Angular measurements of secondary particles

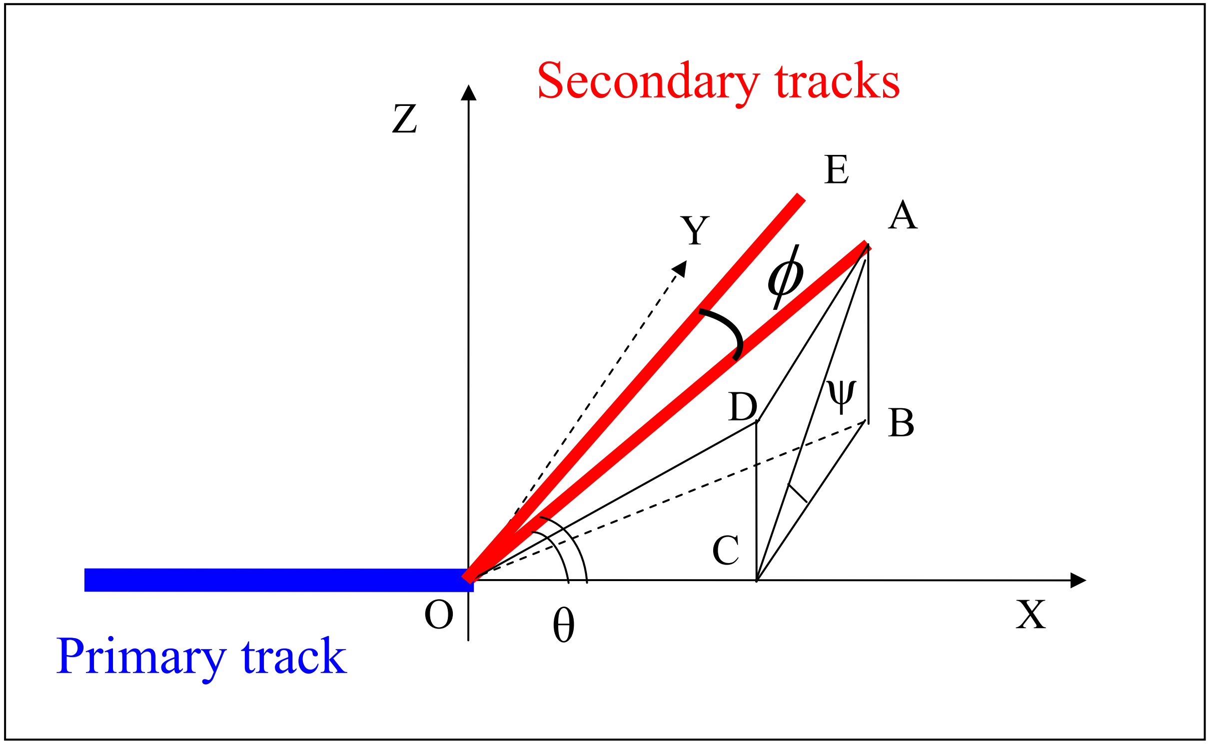

(BOC)	**Emulsion plane**
OX	**Direction of primary track**
$\angle AOC$	**Polar angle** (θ)
$\angle ACB$	**Azimuthal angle** (ψ)
$\angle EOA$	**Opening angle** (ϕ)

Scattering constant

$$K = 11.9\left[1 + 0.837(\log M)^{1/2}\right] \left(\frac{\text{град} \cdot \text{МэВ}}{(100\,\text{мкм})^{1/2}}\right)$$

$$\log M = (const \cdot Z_1^2 t \sum_i (N_i Z_{2i}^2)) - \frac{\sum_i \left\{ N_i Z_{2i}^2 \log Z_{2i}^{2/3} (1 + \frac{Z_1^2 Z_{2i}^2}{0.31 \cdot 137^2}) \right\}}{\sum_i \left\{ N_i Z_{2i}^2 \right\}}$$

Z_1 – the projectile charge (^{14}N)
Z_{2i} – the charge of the target in emulsion
ΣN_i – Σ atom/ cm^3
const – the same for any kind of emulsion

Voyvodic L., Pickup E.// Phys.Rev. 1952. p.85 – 91.

The cross sections calculated within geometric overlap model by the Bradt-Peters formula

- $\lambda_{Ap}=1/\sum_t N_t \sigma_{ApAt}$,

A_p и A_t- the projectile and target mass numbers
σ_{ApAt} – the cross section for projectile-target interaction
N_t – the concentrations of A_t nuclei in the emulsion

- $\sigma_{ApAt}=\pi\, r^2(A_p^{1/3}+ A_t^{1/3}-b^2)$

r =1.23 fm

- $b=1.56—0.2((A_p^{-1/3}+ A_t^{-1/3})$

b – the overlap parameter

Bradt H., Peters B. // Phys. Rev. 1950. V.77. P.54